Analysis of Electron Spin States in Magnetic Fields and Hardware Implementation of Quantum Computers

Yueqian Jiang[1,*] and Zhongzhu Zhu[2]

[1] Keystone Academy, Beijing 101318, China
[2] ChinaBeijing Synchrotron Radiation Facility, Institute of High Energy Physics, Chinese Academy of Sciences, Beijing 100049, China
Email: yueqianleojiang@outlook.com (Y.Q.J.), zhuzz@ihep.ac.cn (Z.Z.Z.)
*Corresponding author
Manuscript received December 4, 2025; accepted January 15, 2025; published February 28, 2026.

***Abstract*—This paper systematically reviews the theoretical progression from blackbody radiation to the foundations of quantum computing. Beginning with Planck's energy quantization and the representation of electromagnetic wave electric field components, the wave-particle duality of photons is analogized to introduce the de Broglie relation between momentum and wave vector for matter waves, leading to the establishment of the matter wave function and the Schrödinger equation as its governing partial differential equation. The consistency between the rigorous solution for a one-dimensional infinitely deep rectangular potential well and the conclusions for a one-dimensional hydrogen atom is demonstrated. Subsequently, within the Dirac notation formalism, the wave function is expressed, and the correspondence between spatial differentiation and momentum is derived, formalizing the momentum operator (often referred to as first quantization). To lay the physical groundwork for manipulating two-qubit states in quantum computing, the potential energy function of an electron's orbital magnetic moment in an external magnetic field is introduced, starting from the torque and work on a current-carrying rectangular coil. This is extended to the magnetic moment and potential energy of a spinning electron, where the orientation of the magnetic field determines the form of the potential and accordingly selects the three components of the Pauli operators. The properties of quantum gates corresponding to the Pauli operators are then examined for single-qubit states. A two-qubit state, constructed via the coupling of two arbitrary single-qubit states represented in a two-level system or electron spin, is shown to be uniquely expressible as a superposition of four eigen two-qubit states. The paper further investigates joint manipulations of two-qubit states, including evolution under X and Z gates conditioned on high- and low-level states, the representation of control-flow circuits (with the low-level as control), and the formulation of measurement and CNOT gates. Throughout this work, essential mathematical tools—including integration, matrix operations, complex Euler's formula, and solutions to simple second-order ordinary differential equations—are incorporated to provide a coherent theoretical framework for state representation and gate operations in quantum computing.**

***Keywords*—Blackbody, quantum state, magnetic moment, potential field, quantum computing, dual bit state**

I. Introduction

Quantum computing heralds a paradigm shift in information processing by harnessing the principles of quantum mechanics—superposition, entanglement, and interference—to solve problems intractable for classical computers [1]. While its theoretical foundations were laid in the early 1980s, the field has evolved from a purely conceptual discipline into a intense global scientific and engineering pursuit, driven by its potential to revolutionize cryptography, materials science, drug discovery, and artificial intelligence [1–3].

The core of this potential lies in the quantum bit (qubit). Unlike a classical bit, a qubit can exist in a superposition of both $|0\rangle$and $|1\rangle$states simultaneously. When multiple qubits are entangled, a quantum computer can process a vast number of possibilities in parallel [4]. This computational advantage is exemplified by Shor's algorithm for integer factorization, which threatens current cryptographic protocols, and Grover's algorithm for unstructured search, which provides a quadratic speedup [5].

However, the path to practical quantum computing is fraught with fundamental challenges. Qubits are notoriously fragile, susceptible to decoherence and environmental noise that introduce errors [6]. Consequently, current quantum processors operate in the Noisy Intermediate-Scale Quantum (NISQ) era, characterized by devices with limited qubit counts that lack full fault-tolerance [7]. A significant research focus is therefore on Quantum Error Correction (QEC) codes and fault-tolerant architectures to detect and correct errors, which are prerequisites for large-scale, reliable quantum computation [8].

The hardware landscape is diverse, with several competing platforms—including superconducting circuits [9], trapped ions [10], photonic systems, and topological qubits—vying for dominance based on coherence times, gate fidelities, and scalability. Recent progress has focused on increasing qubit counts, improving gate fidelities beyond the error correction threshold, and demonstrating quantum advantage for specific tasks [11].

Complementing these hardware advances, the development of quantum algorithms continues to expand into areas such as quantum chemistry, optimization, and machine learning [12]. Furthermore, the creation of accessible software stacks, programming languages like Qiskit and Cirq, and quantum cloud platforms is crucial for broadening community engagement and application development [13].

In summary, while rapid advancements in hardware, error mitigation, algorithms, and software are driving the field forward, the persistent challenges of noise and scalability in the NISQ era define the current research frontier. This work aiming to address key obstacles towards the practical realization of quantum computational advantage.

DOI: 10.7763/IJET.2026.V18.1336

II. METHODOLOGY

A. From Blackbody Radiation to the Schrödinger Equation

The classical Rayleigh-Jeans law, derived from the equipartition theorem applied to the standing electromagnetic modes within a cavity, predicted a spectral energy density $u(\nu, T) \propto \nu^2$ that diverged at high frequencies—the so-called "ultraviolet catastrophe." This was in stark contradiction to experimental observations. In 1900, Max Planck resolved this paradox by introducing a radical postulate: the energy exchange between the cavity walls and the radiation field is not continuous but quantized. He proposed that the energy of a mode with frequency ν is restricted to integer multiples of a fundamental quantum, $E_n = nh\nu$, where n is a positive integer and h is Plancks constant.

This quantization can be rigorously derived by considering the boundary conditions for electromagnetic waves in a cavity of volume $V = L_x L_y L_z$. The allowed wavevectors are $\vec{k} = (2\pi n_x/L_x, 2\pi n_y/L_y, 2\pi n_z/L_z)$, where n_i are positive integers. Counting the number of modes with wavevector magnitude between k and $k + dk$ in the positive octant yields the density of states in k-space. Transforming this to frequency space via $k = 2\pi\nu/c$ gives the number of modes per unit volume per unit frequency:

$$N(\nu)d\nu = \frac{8\pi\nu^2}{c^3}d\nu \tag{1}$$

In classical statistical mechanics, the average energy per mode at temperature T is $k_B T$, leading directly to the divergent Rayleigh-Jeans law. Plancks quantum hypothesis modifies this calculation. The partition function for a single quantized harmonic oscillator becomes a geometric series:

$$Z = \sum_{n=0}^{\infty} e^{-nh\nu/k_B T} = \frac{1}{1-e^{-h\nu/k_B T}} \tag{2}$$

The mean energy is then $\langle E\rangle = -\frac{\partial \ln Z}{\partial \beta} = \frac{h\nu}{e^{h\nu/k_B T}-1}$. Combining this with the mode density $N(\nu)$ yields Plancks celebrated distribution:

$$u(\nu, T) = \frac{8\pi h\nu^3}{c^3}\frac{1}{e^{h\nu/k_B T}-1} \tag{3}$$

which accurately describes the experimental spectrum across all frequencies, as shown in Fig. 1.

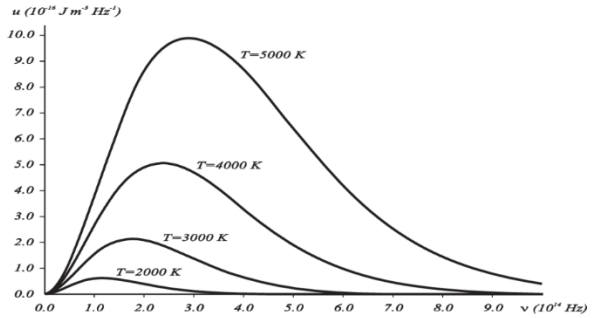

Fig. 1. Spectral energy density $u(\nu, T)$ of blackbody radiation at different temperatures as a function of the frequency ν.

The wave-particle duality, postulated by Louis de Broglie in 1924, extended the quantum concept to matter. He associated a wavelength $\lambda = h/p$ with a particle of momentum p, formally linking the particle properties (energy E and momentum $\vec{p}$) to wave properties (angular frequency ω and wavevector $\vec{k}$) via $\vec{p} = \hbar\vec{k}$ and $E = \hbar\omega$. A monochromatic plane wave solution of the classical wave equation, $e^{i(\vec{k}\cdot\vec{r}-\omega t)}$, can thus be reinterpreted as a matter wave for a free particle:

$$\Psi(\vec{r}, t) = Ae^{\frac{i}{\hbar}(\vec{p}\cdot\vec{r}-Et)} \tag{4}$$

Differentiating this wave function reveals fundamental operator correspondences:

$$i\hbar\frac{\partial}{\partial t}\Psi = E\Psi \quad \text{and} \quad -i\hbar\nabla\Psi = \vec{p}\Psi \tag{5}$$

This suggests the identifications $\hat{E} \equiv i\hbar\frac{\partial}{\partial t}$ and $\hat{\vec{p}} \equiv -i\hbar\nabla$. For a non-relativistic particle with total energy $E = \frac{p^2}{2m} + V(\vec{r})$, substituting the operators leads to the time-dependent Schrödinger equation:

$$i\hbar\frac{\partial}{\partial t}\Psi(\vec{r}, t) = \left[-\frac{\hbar^2}{2m}\nabla^2 + V(\vec{r})\right]\Psi(\vec{r}, t) \tag{6}$$

For stationary states with definite energy E, where $\Psi(\vec{r}, t) = \psi(\vec{r})e^{-iEt/\hbar}$, we obtain the time-independent Schrödinger equation:

$$\left[-\frac{\hbar^2}{2m}\nabla^2 + V(\vec{r})\right]\psi(\vec{r}) = E\psi(\vec{r}) \tag{7}$$

which is an eigenvalue equation for the Hamiltonian operator $\hat{H}$.

B. Quantum Bound States: The Infinite Potential Well

The one-dimensional infinite potential well, or "particle in a box," is a paradigmatic exactly solvable model that illustrates the quintessential quantum phenomena of energy quantization and zero-point energy. It models a particle confined to a region $0 < x < a$ by an impenetrable potential: $V(x) = 0$ inside and $V(x) = \infty$ outside. The infinite potential enforces the boundary condition that the wavefunction must vanish at the walls: $\psi(0) = \psi(a) = 0$.

Within the well, the time-independent Schrödinger equation simplifies to that of a free particle:

$$-\frac{\hbar^2}{2m}\frac{d^2\psi}{dx^2} = E\psi \tag{8}$$

Defining $k = \sqrt{2mE}/\hbar$, the general solution is $\psi(x) = A\sin(kx) + B\cos(kx)$. The boundary condition $\psi(0) = 0$ forces $B = 0$. The condition $\psi(a) = 0$ then requires $ka = n\pi$, where $n = 1,2,3,\ldots$. This leads to the quantization of the wavevector, $k_n = n\pi/a$, and consequently the energy:

$$E_n = \frac{\hbar^2 k_n^2}{2m} = \frac{n^2\pi^2\hbar^2}{2ma^2} \tag{9}$$

The corresponding normalized eigenfunctions are

$$\psi_n(x) = \sqrt{\frac{2}{a}}\sin\left(\frac{n\pi x}{a}\right) \tag{10}$$

These solutions, depicted in Fig. 2, reveal key features: (1) The ground state energy $E_1 > 0$ signifies zero-point motion. (2) The energy levels scale quadratically with the quantum number n. (3) The eigenfunctions are mutually orthogonal and form a complete basis for the Hilbert space of square-integrable functions on the interval $[0, a]$.

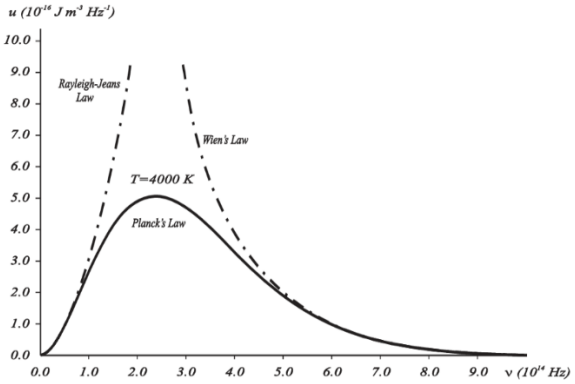

Fig. 2 Comparison of various spectral densities: while the Planck and experimental distributions match perfectly (solid curve), the Rayleigh–Jeans and the Wien distributions (dotted curves) agree only partially with the experimental distribution.

This formalism is elegantly captured in Diracs bra-ket notation. A physical state is represented by a ket $|\psi\rangle$ in an abstract Hilbert space. The eigenstates of the Hamiltonian satisfy $\hat{H}|\phi_n\rangle = E_n|\phi_n\rangle$. A general state of the isolated system can be expressed as a coherent superposition of these eigenstates: $|\psi\rangle = \sum_n c_n|\phi_n\rangle$, where the complex coefficients c_n satisfy $\sum_n |c_n|^2 = 1$. The expectation value of an observable $\hat{O}$ in such a state is $\langle\hat{O}\rangle = \langle\psi|\hat{O}|\psi\rangle$.

The coordinates of three nodes E, F and G are known as (xe, ye), (xf, yf) and (xg, yg). And the distance from them to the unknown node M is de, df and dg, respectively. Set the coordinate of unknown node M to (x, y), then from (2), (x, y) can be calculated and obtained.

III. Results and Discussion

A. Deriving the Potential Energy Function of Electron Spin Magnetic Moment in a Magnetic Field from the Work Done by the Current Carrying Coil Magnetic Moment in a Magnetic Field

The interaction of magnetic moments with external fields provides a crucial physical mechanism for manipulating quantum states, particularly in quantum computing implementations. The classical model starts with a planar current loop of area $\vec{A}$ (magnitude A, direction normal to the plane). Its magnetic dipole moment is $\vec{\mu} = I\vec{A}$. In a uniform magnetic field $\vec{B}$, the loop experiences a torque $\vec{\tau} = \vec{\mu} \times \vec{B}$, which seeks to align $\vec{\mu}$ with $\vec{B}$. The potential energy associated with the orientation θ between $\vec{\mu}$ and $\vec{B}$ is the negative line integral of the torque:

$$U = -\int \vec{\tau} \cdot d\vec{\theta} = -\vec{\mu} \cdot \vec{B} \qquad (11)$$

For an electron in a circular Bohr orbit, the magnetic moment arises from its orbital motion. The current is $I = -e/T$, where T is the orbital period. With area $A = \pi r^2$ and angular momentum $L = m_e v r = m_e \omega r^2$, the orbital magnetic moment becomes:

$$|\vec{\mu}_L| = IA = \left(\frac{-e}{2\pi/\omega}\right)(\pi r^2) = -\frac{e}{2m_e}L \qquad (12)$$

Considering direction ($\vec{\mu}_L$ is opposite to $\vec{L}$ for a negative charge), the vector relation is:

$$\vec{\mu}_L = -\frac{g_L e}{2m_e}\vec{L} \qquad (13)$$

where $g_L = 1$ is the orbital g-factor. Hence, the potential energy for an orbiting electron in a field is $U_L = -\vec{\mu}_L \cdot \vec{B} = \frac{g_L e}{2m_e}\vec{L} \cdot \vec{B}$.

Electrons possess an intrinsic angular momentum called spin, $\vec{S}$, with no classical analogue. Remarkably, it also carries a magnetic moment. By analogy with orbital motion, we write:

$$\vec{\mu}_S = -\frac{g_s e}{2m_e}\vec{S} \qquad (14)$$

where experiment dictates the spin g-factor $g_s \approx 2.0023 \approx 2$. In quantum mechanics, spin is an internal degree of freedom described by the Pauli spin matrices. For a spin-1/2 particle like the electron, $\vec{S} = (\hbar/2)\vec{\sigma}$, where $\vec{\sigma} = (\sigma_x, \sigma_y, \sigma_z)$ are the Pauli matrices. The interaction Hamiltonian for the spin magnetic moment in a field $\vec{B} = B\hat{n}$ is therefore:

$$\hat{H}_S = -\vec{\mu}_S \cdot \vec{B} = \frac{g_s e\hbar}{4m_e}(\vec{\sigma} \cdot \hat{n})B = \frac{\hbar\omega_L}{2}\vec{\sigma} \cdot \hat{n} \qquad (15)$$

where $\omega_L = g_s eB/(2m_e)$ is the Larmor frequency.

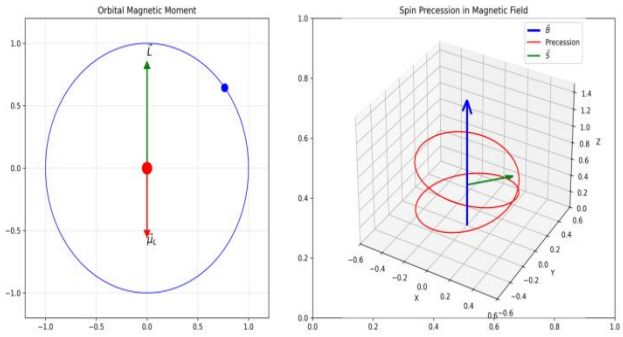

Fig 3. Magnetic moment dynamics. (Left) Orbital motion generates a magnetic moment μ_L anti-parallel to its angular momentum L. (Right) A spin magnetic moment μ_S precesses around an applied magnetic field B.

As shown in Fig. 3, this Hamiltonian causes the spin state to precess around the field direction. By choosing $\hat{n}$ to be along the x-, y-, or z-axis, the interaction Hamiltonian becomes proportional to σ_x, σ_y or σ_z, respectively. These Pauli operators, given by

$$\sigma_x = \begin{pmatrix} 0 & 1 \\ 1 & 0 \end{pmatrix}, \sigma_y = \begin{pmatrix} 0 & -i \\ i & 0 \end{pmatrix}, \sigma_z = \begin{pmatrix} 1 & 0 \\ 0 & -1 \end{pmatrix} \qquad (16)$$

are Hermitian, traceless, and satisfy the algebra $[\sigma_i, \sigma_j] = 2i\epsilon_{ijk}\sigma_k$. They form the foundational set for single-qubit rotations in quantum computing, physically realized by applying precisely controlled magnetic field pulses.

B. Quantum Computation: States, Gates, and Measurement

The fundamental unit of quantum information is the quantum bit or qubit. Its state resides in a two-dimensional complex Hilbert space, spanned by the orthonormal computational basis states $\{|0\rangle, |1\rangle\}$, often corresponding to spin-up and spin-down eigenstates of σ_z. A pure state of a single qubit is a coherent superposition:

$$|\psi\rangle = \alpha|0\rangle + \beta|1\rangle, \quad \alpha, \beta \in \mathbb{C} \qquad (17)$$

with the normalization condition $|\alpha|^2 + |\beta|^2 = 1$. This state can be visualized as a point on the Bloch sphere, parameterized as $|\psi\rangle = \cos(\theta/2)|0\rangle + e^{i\phi}\sin(\theta/2)|1\rangle$.

The Pauli matrices, derived from physical spin interactions, serve as fundamental quantum logic gates. Their action on the basis states is:

$$X \equiv \sigma_x: |0\rangle \leftrightarrow |1\rangle \quad \text{(bit-flip)},$$
$$Y \equiv \sigma_y: |0\rangle \to i|1\rangle, |1\rangle \to -i|0\rangle, \tag{18}$$
$$Z \equiv \sigma_z: |0\rangle \to |0\rangle, |1\rangle \to -|1\rangle \text{(phase-flip)}.$$

Another crucial single-qubit gate is the Hadamard gate,

$$H = \frac{1}{\sqrt{2}}\begin{pmatrix} 1 & 1 \\ 1 & -1 \end{pmatrix} \tag{19}$$

which creates superpositions: $H|0\rangle = |+\rangle = (|0\rangle + |1\rangle)/\sqrt{2}$ and $H|1\rangle = |-\rangle = (|0\rangle - |1\rangle)/\sqrt{2}$. These gate matrices are unitary, ensuring they preserve the norm of the quantum state.

A multi-qubit system is described by the tensor product of the individual Hilbert spaces. For two qubits in states $|\psi\rangle_A$ and $|\phi\rangle_B$, the composite state is $|\Psi\rangle_{AB} = |\psi\rangle_A \otimes |\phi\rangle_B$. If the individual states are superpositions, the tensor product yields entangled states that cannot be written as a simple product. The two-qubit computational basis is $\{|00\rangle, |01\rangle, |10\rangle, |11\rangle\}$. A general two-qubit state is:

$$|\Psi\rangle = c_{00}|00\rangle + c_{01}|01\rangle + c_{10}|10\rangle + c_{11}|11\rangle, \quad \sum_{i,j\in\{0,1\}} |c_{ij}|^2 = 1 \tag{20}$$

Multi-qubit gates are constructed via tensor products of single-qubit gates and controlled operations. A cornerstone for entangling qubits is the controlled-NOT (CNOT) gate. It acts on two qubits: a control and a target. Its matrix representation (for control on qubit 1 and target on qubit 2) is:

$$\text{CNOT} = \begin{pmatrix} 1 & 0 & 0 & 0 \\ 0 & 1 & 0 & 0 \\ 0 & 0 & 0 & 1 \\ 0 & 0 & 1 & 0 \end{pmatrix} \tag{21}$$

Its action is: if the control is $|0\rangle$, the target is left unchanged; if the control is $|1\rangle$, an X gate is applied to the target: $|c, t\rangle \to |c, t \oplus c\rangle$. This gate can generate maximal entanglement, e.g., $\text{CNOT}(|+\rangle|0\rangle) = (|00\rangle + |11\rangle)/\sqrt{2}$. The role of control and target can be swapped, leading to a different matrix. Fig. 4 illustrates a quantum circuit combining single- and two-qubit gates.

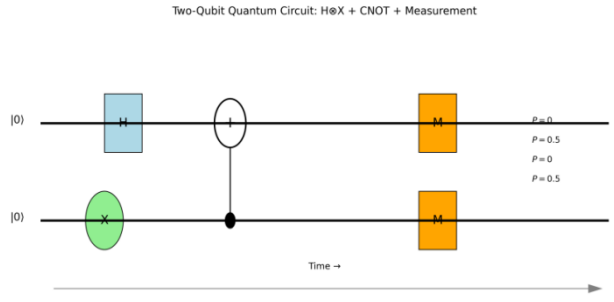

Fig. 4. A two-qubit quantum circuit. The circuit implements the sequence (H⊗X) followed by a CNOT on the initial state $|00\rangle$, followed by measurement gates (M).

The final, non-unitary step in a quantum algorithm is measurement, which projects a quantum state onto a classical outcome. According to the Born rule, a projective measurement is described by a set of Hermitian operators $\{M_m\}$, where m labels a possible outcome, satisfying $\sum_m M_m^\dagger M_m = I$. For a measurement in the computational basis, $M_m = |m\rangle\langle m|$. The probability of obtaining outcome m when measuring state $|\psi\rangle$ is:

$$p(m) = \langle\psi|M_m^\dagger M_m|\psi\rangle = |\langle m|\psi\rangle|^2 \tag{22}$$

Given outcome m, the post-measurement state collapses to:

$$|\psi'\rangle = \frac{M_m|\psi\rangle}{\sqrt{p(m)}}.$$

For a two-qubit state, the measurement operators are $M_{00}, M_{01}, M_{10}, M_{11}$. The statistics of repeated measurements on identically prepared states reveal the squared magnitudes of the superposition coefficients, as demonstrated in Fig. 5.

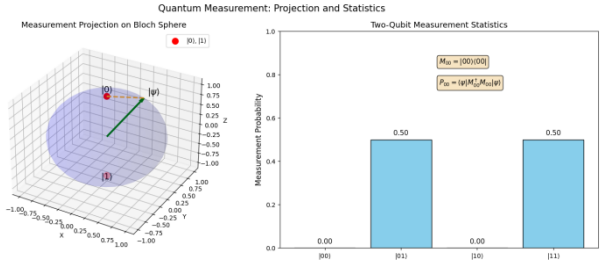

Fig. 5. Quantum measurement. (Left) On the Bloch sphere, measurement projects a general state $|\psi\rangle$ (green arrow) onto one of the basis states $|0\rangle$ or $|1\rangle$ (red points). (Right) The resulting statistical distribution for a two-qubit measurement, showing probabilities for each basis outcome.

IV. Conclusion

This study systematically constructs a comprehensive theoretical framework that connects the fundamental principles of quantum mechanics to the core operations of quantum computing. It begins with the theories of blackbody radiation and electromagnetic waves, introducing the concept of the matter-wave function and establishing the dynamical rules for its evolution via the Schrödinger equation. The formal foundations are completed through the canonical "first" quantization of momentum, corresponding it to the spatial gradient operator. The fundamental principle that the superposition state of an isolated quantum system can be linearly expressed by its eigenstates is thus established.

Subsequently, the research proceeds from the classical electromagnetic principles of torque and work performed on a current-carrying coil in an external magnetic field to derive the potential energy function for an electron's orbital magnetic moment. By drawing an analogy between electron spin and an "equivalent" orbital magnetic moment, this potential energy model is extended to spin systems, thereby establishing the mechanical and energetic description of a spin magnetic moment in a magnetic field. The analysis indicates that tuning the magnetic field direction selects the specific form of the potential energy function, which corresponds physically to the three components of the Pauli operators, laying the theoretical groundwork for the physical manipulation of two-qubit states in quantum computing.

The study then transitions to the concrete implementation of quantum computing. Starting from a single-qubit state, it systematically analyzes the properties of the three

fundamental quantum gates (X, Y, Z) corresponding to the Pauli operators. For a two-qubit system, a description using a two-level structure or a two-electron spin system is employed. It is demonstrated that any two-qubit state formed from the tensor product construction rule of two arbitrary single-qubit states can be uniquely represented as a linear superposition of four eigen two-qubit states. The critical functions of the Hadamard (H) and CNOT gates, along with the mathematical formulation of the measurement gate, are further examined. Finally, via a specific two-qubit quantum circuit example, the study explicitly calculates the state evolution under a sequence of gate operations and the subsequent measurement outcome, providing a complete demonstration of the fundamental quantum computation workflow.

Conflict of Interest

The authors declare no conflict of interest.

Author Contributions

Yueqian Jiang performed the primary research, processed the data, and prepared the figures; Yueqian Jiang also wrote the initial draft of the manuscript ; Zhongzhu Zhu provided supervision, reviewed the analysis, and performed the final editing and revision of the paper ; all authors have read and agreed to the published version of the manuscript.

References

[1] M. A. Nielsen and I. L. Chuang, *Quantum Computation and Quantum Information: 10th Anniversary Edition*, Cambridge University Press, 2010.

[2] D. Castelvecchi, "Quantum computers: What are they good for?" *Nature*, vol. 617(7962), S1–S3, 2023.

[3] P. W. Shor, "Algorithms for quantum computation: discrete logarithms and factoring," in *Proc. 35th Annual Symposium on Foundations of Computer Science*, 1994, pp. 124–134.

[4] R. P. Feynman, "Simulating physics with computers," *International Journal of Theoretical Physics*, vol. 21 (6/7), pp. 467–488, 1982.

[5] J. Preskill, Quantum computing and the entanglement frontier. arXiv preprint arXiv:1203.5813, 2012.

[6] M. H. Devoret and R. J. Schoelkopf, "Superconducting circuits for quantum information: an outlook," *Science*, vol. 339 (6124), pp. 1169–1174, 2013.

[7] F. Arute *et al.*, "Quantum supremacy using a programmable superconducting processor," *Nature*, vol. 574 (7779), pp. 505–510, 2019.

[8] J. Biamonte *et al.*, "Quantum machine learning," *Nature*, vol. 549(7671), pp. 195–202, 2017.

[9] T. Häner et al., "A software methodology for compiling quantum programs," *Quantum Science and Technology*, vol. 3, no. 2, 020501, 2018.

[10] J. Preskill, "Quantum computing in the NISQ era and beyond," *Quantum*, vol. 2, p. 79, 2018.

[11] C. D. Bruzewicz et al., "Trapped-ion quantum computing: Progress and challenges," *Applied Physics Reviews*, vol. 6, no. 2, 021314, 2019.

[12] H. J. Kimble, "The quantum internet," *Nature*, vol. 453, no. 7198, pp. 1023–1030, 2008.

[13] S. Endo *et al.*, "Hybrid quantum-classical algorithms and quantum error mitigation," *Journal of the Physical Society of Japan*, vol. 90, no. 3, 032001, 2021.